High-Pressure Phase Diagrams of Methane + 1,2,3,4-Tetrahydronaphthalene and Methane + 9,10-Dihydrophenanthrene Mixtures

P. Tobaly* and P. Marteau

Laboratoire d'Ingéniérie des Matériaux et des Hautes Pressions, CNRS, Institut Galilée, 93430 Villetaneuse, France

V. Ruffier-Meray

Institut Français du Pétrole, 1 and 4 Avenue de Bois Préau, 92852 Rueil-Malmaison, France

Equilibrium data on the methane + 1,2,3,4-tetrahydronaphthalene (tetralin) mixture at (294, 323, 373, and 423) K and on the methane + 9,10-dihydrophenanthrene mixture at (423 and 463) K are reported. The data have been obtained with a high-pressure cell and an infrared absorption method previously described.

Introduction

This work is part of a continuing effort to increase knowledge about thermodynamic properties of crude oils and natural gases. It is of major importance to be able to calculate thermodynamic behavior of crude oils at all conditions encountered during petroleum processing. Usually, equations of state are used to perform these calculations, and binary interaction parameters are used by these models to predict multicomponent properties. If group contribution methods are used to calculate properties of those complex mixtures, then specific parameters relative to the interactions between groups of the molecules are needed. Similarly, if molecular simulation is used, parameters of the potentials must take into account the interactions between different molecules or groups. To calculate these parameters, experimental data on binary mixtures are necessary. We have been involved for many years in the experimental determination of phase diagrams of binary mixtures. Data for methane + 1-methylnaphthalene (Marteau et al., 1996), methane + hexane and methane + benzene (Marteau et al., 1997), and methane + squalane and methane + hexatriacontane (Marteau et al., 1998) mixtures have been previously published. Two new binary mixtures have been investigated, methane + tetralin (1,2,3,4-tetrahydronaphthalene) and methane + 9,10-dihydrophenanthrene. Results are presented hereafter.

Experimental Section

Materials. The purity of methane was 99.9%. Tetralin was obtained fom Aldrich with a purity of 99%. The purity of 9,10-dihydrophenanthrene (from Lancaster) was only 97%. Two other suppliers offer material with a purity of 94 and 95%. The purification of 9,10-dihydrophenanthrene seems to be so difficult that it can be assumed that the remaining impurities must be of a very similar nature. All compounds were used as is without further purification. The apparatus and experimental procedure have been previously described (Marteau et al., 1996). Concentration measurements of each component in the gas and liquid phases have been obtained with an accuracy better than 1%, as mentioned in the preceding paper (Marteau et al., 1998). The concentration of methane which remains high enough in both phases is easily measured with this accuracy. As for the other molecule, its concentration may be very low in the gas phase. Therefore, concentration measurements in the gas phase at low pressure are not reported because of too-low infrared absorption by the solute. Although measurable absorption could be obtained by increasing the absorption path length, it has not been done since measurements in this pressure range can be easily obtained using more classical methods. The relative

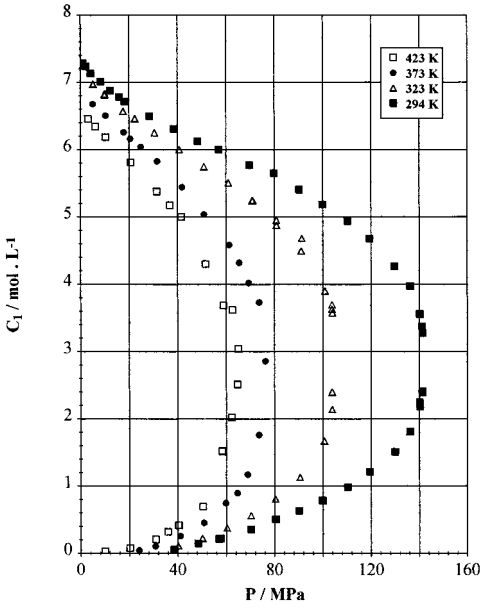

Figure 1. Concentration of tetralin as a function of pressure in the gas and liquid coexisting phases for the mixture tetralin + methane at four temperatures (■, 294 K; △, 323 K; ●, 373 K; □, 423 K).

* To whom all correspondence should be addressed. E-mail: tobaly@limhp.univ-paris 13.fr.

10.1021/je990045j CCC: $18.00
Published on Web 10/28/1999

Table 1. Vapor−Liquid Equilibrium Data for Tetraline + Methane at (294, 323, 373, and 423) K (C_1 = Tetralin Concentration; C_2 = Methane Concentration)

	gas phase		liquid phase			gas phase		liquid phase	
P/MPa	C_1/(mol·L^{-1})	C_2/(mol·L^{-1})	C_1/(mol·L^{-1})	C_2/(mol·L^{-1})	P/MPa	C_1/(mol·L^{-1})	C_2/(mol·L^{-1})	C_1/(mol·L^{-1})	C_2/(mol·L^{-1})
				T = 294 K					
1.0			7.286	0.289	80.1	0.504	18.951	5.649	6.218
2.1			7.234	0.437	90.2	0.634	19.220	5.405	7.230
4.2			7.131	0.806	99.9	0.786	19.309	5.186	7.986
8.3			7.010	1.323	110.2	0.984	19.275	4.937	8.875
12.2			6.872	1.770	119.4	1.213	19.010	4.676	9.803
16.0			6.783	2.099	129.8	1.511	18.635	4.269	11.122
18.2			6.710	2.126	136.2	1.807	17.988	3.973	12.057
28.4			6.495	2.909	140.1	2.248	17.114	3.565	13.503
38.4	0.056	15.290	6.311	3.656	140.3	2.192	17.016	3.553	13.266
48.4	0.146	16.708	6.123	4.322	140.3	2.180	17.017		
57.0	0.215	17.580	6.001	4.891	141.2	2.391	16.555	3.373	13.850
57.6	0.222	17.675			141.4	2.413	16.484	3.277	14.058
70.0	0.353	18.494	5.770	5.721					
				T = 323 K					
5.2			6.975	0.724	70.6	0.563	17.110	5.248	6.946
5.2			6.967	0.773	70.9			5.251	6.907
10.0			6.814	1.315	70.9			5.241	7.015
10.0			6.829	1.336	80.6	0.810	17.465	4.876	7.891
17.5			6.572	2.136	80.8			4.951	7.957
22.3			6.463	2.578	90.8	1.132	17.496	4.497	9.220
22.4			6.464	2.559	91.3			4.683	8.868
22.4			6.457	2.591	100.8	1.672	16.745	3.903	11.096
30.3			6.251	3.364	103.8	2.143	15.780	3.700	11.874
40.4	0.112	14.110	6.003	4.246	103.8	2.400	15.060	3.634	12.023
50.5	0.224	15.526	5.748	5.106	103.9			3.580	12.169
60.7	0.380	16.511	5.509	6.028					
				T = 373 K					
5.1			6.675	0.624	50.9	0.454	13.120	5.036	5.969
10.4			6.503	1.234	60.0	0.748	13.947	4.584	7.367
17.6			6.254	2.064	65.0	0.896	14.481	4.320	8.096
20.3			6.160	2.327	69.1	1.171	14.274	4.019	8.861
24.5	0.041	7.864	6.039	2.864	73.6	1.761	13.610	3.732	9.631
31.2	0.104	9.702	5.824	3.587	76.2			2.859	11.734
41.4	0.257	11.937	5.440	4.815					
				T = 423 K					
3.1			6.455	0.379	40.9	0.417	10.324	5.001	4.909
6.1			6.340	0.738	51.0	0.696	11.988	4.301	6.963
10.2	0.027	3.007	6.184	1.230	58.6	1.526	11.793	3.686	8.352
20.5	0.079	5.855	5.811	2.496	58.4	1.513	11.848		
31.1	0.206	8.383	5.378	3.855	62.4	2.022	11.450	3.620	8.804
36.3	0.321	9.526	5.176	4.627	64.9	2.514	10.699	3.041	9.939

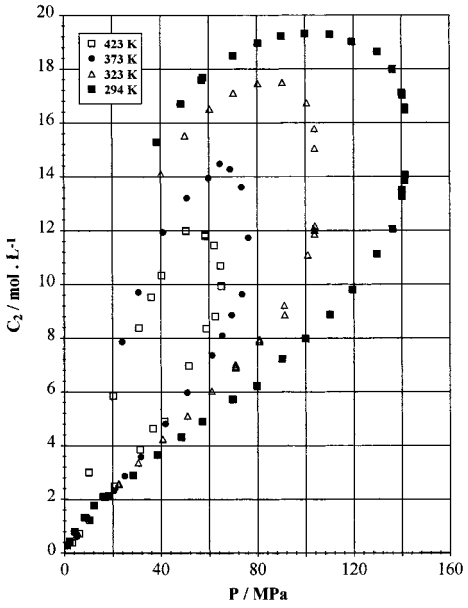

Figure 2. Concentration of methane as a function of pressure in the gas and liquid coexisting phases for the mixture tetralin + methane at four temperatures (■, 294 K; △, 323 K; ●, 373 K; □, 423 K).

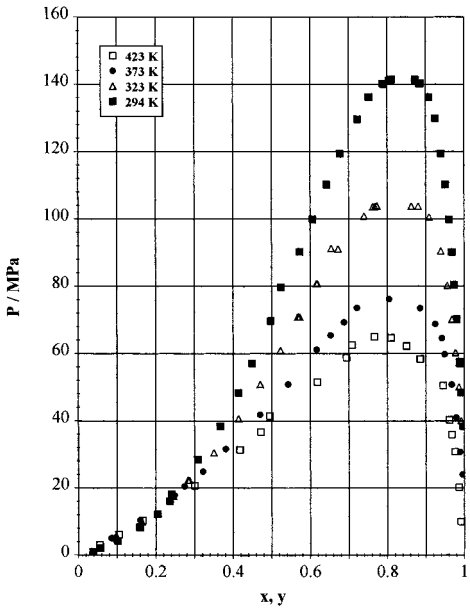

Figure 3. Phase diagrams of tetralin + methane at four temperatures (■, 294 K; △, 323 K; ●, 373 K; □, 423 K). x, y = $C_2/(C_1 + C_2)$ = mole fractions of methane.

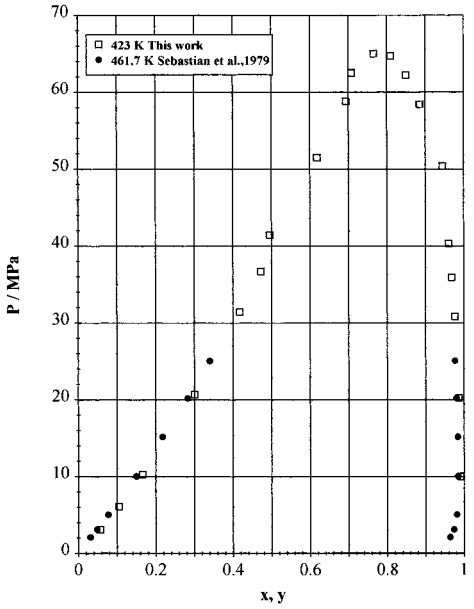

Figure 4. Phase diagram of tetralin + methane (□, this work, 423 K; ●, Sebastian et al. (1979), 461.7. $x, y = C_2/(C_1 + C_2)$ = mole fractions of methane.

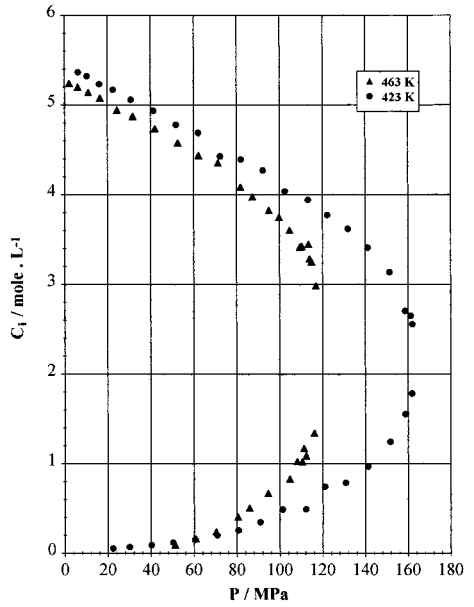

Figure 5. Concentration of 9,10-dihydrophenanthrene as a function of pressure in the gas and liquid coexisting phases for the mixture 9,10-dihydrophenanthrene + methane at (●) 423 K and (▲) 463 K.

uncertainty on the mole fraction may be computed by

$$\frac{\Delta y}{y} = 2\frac{\Delta c}{c}(1 - y) \qquad (1)$$

where $\Delta c/c$ is the relative uncertainty for concentration measurements. As a result, $\Delta y/y$ is always lower or equal to $2\Delta c/c$ even if the concentration of the minor component goes to zero.

Here again the most important source of uncertainty is the pressure gauge with an accuracy of 0.4 MPa.

Results

Methane + Tetralin Mixture. Vapor−liquid equilibrium data for the methane + tetralin mixture are reported in Table 1. Tetralin (C_1) and methane (C_2) concentrations

Table 2. Vapor−Liquid Equilibrium Data for 9,10-Dihydrophenanthrene + Methane at (423 and 463) K (C_1 = 9,10-Dihydrophenanthrene Concentration; C_2 = Methane Concentration)

	gas phase		liquid phase	
P/MPa	C_1/(mol·L^{-1})	C_2/(mol·L^{-1})	C_1/(mol·L^{-1})	C_2/(mol·L^{-1})
		T = 423 K		
6.3			5.365	0.372
10.4			5.320	0.653
16.2			5.231	0.995
22.4	0.053	6.347	5.169	1.386
30.4	0.068	8.363	5.057	1.932
40.8	0.092	10.425	4.935	2.616
51.1	0.117	12.127	4.779	3.161
61.3	0.153	13.460	4.690	3.801
71.5	0.200	14.545	4.427	4.503
81.4	0.257	15.318	4.394	4.933
91.6	0.346	15.991	4.268	5.576
101.9	0.489	16.648	4.036	6.351
112.7	0.494	16.842	3.941	6.978
121.6	0.745	16.842	3.773	7.709
131.3	0.787	17.111	3.617	8.343
141.2	0.970	16.878	3.410	9.196
151.5	1.243	16.492	3.136	10.357
158.7	1.553	15.852	2.705	11.937
161.2			2.650	12.127
161.8	1.784	15.078	2.554	12.563
		T = 463 K		
2.2			5.242	0.123
6.2			5.202	0.372
11.0			5.145	0.705
16.5			5.078	1.104
24.2			4.944	1.616
31.4			4.874	2.204
41.6			4.738	2.838
51.9	0.094	11.305	4.579	3.516
61.6	0.164	12.469	4.439	4.168
70.9	0.242	13.363	4.356	4.808
81.1	0.406	14.148	4.087	5.742
86.6	0.511	14.414	3.976	6.063
94.8	0.670	14.591	3.825	6.783
99.8			3.748	6.917
104.6	0.832	14.856	3.606	7.575
108.8	1.028	14.571	3.417	8.189
110.4	1.025	14.342	3.424	8.029
111.7	1.171	14.474		
112.9	1.089	14.454	3.449	8.302
113.9			3.284	8.666
114.9			3.253	8.658
116.5	1.345	14.233	2.984	9.609

in each phase are given at various pressures. Other quantities such as mole fraction and molar volume may be determined from these data. Figures 1 and 2 show plots of tetralin and methane concentrations as a function of pressure along the coexistence lines. Pressure−mole fraction plots at (294, 323, 373, and 423) K including the critical vicinity are shown in Figure 3.

Notice that, in this temperature range, the mixture critical pressure decreases with increasing temperature. This may be discussed in view of the classical classification of phase diagrams for binary mixtures (Van Konynenburg and Scott, 1980). In all types of phase diagrams except for type III the critical line exhibits a maximum in pressure and decreases toward the critical point of the heavier component. Such a maximum in pressure, if it exists, is expected to lie at a lower temperature. It is a common feature of these diagrams that the maximum in pressure is found at temperatures closer to the light component critical temperature (here 190 K) than to the heavier one (here 716 K). Figure 4 shows a comparison of our data at 423 K with those reported by Sebastian et al. (1979) at 461 K. Though at different temperatures, the data may be compared because, as may be seen in Figure 3, the data at

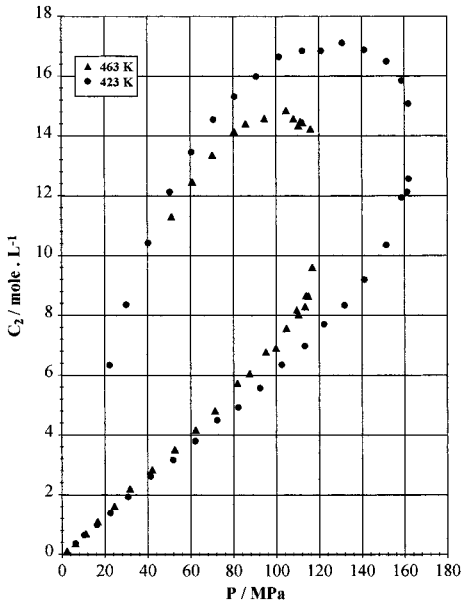

Figure 6. Concentration of methane as a function of pressure in the gas and liquid coexisting phases for the mixture 9,10-dihydrophenanthrene + methane at (●) 423 K and (▲) 463 K.

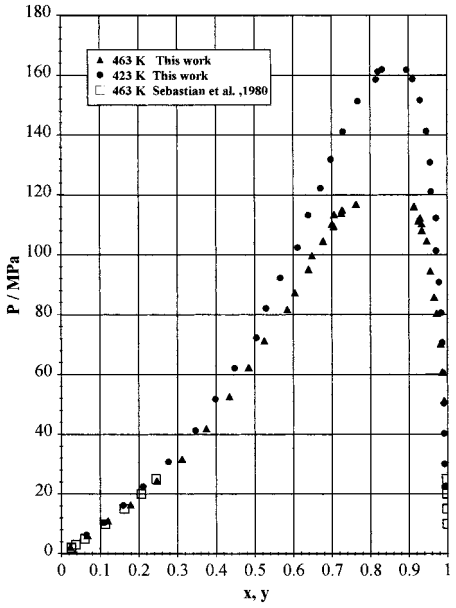

Figure 7. Phase diagram of 9,10-dihydrophenanthrene + methane at two temperatures (●) 423 K and (▲) 463 K, this work; and (□) 463 K, Sebastian et al. (1980). x, $y = C_2/(C_1 + C_2)$ = mole fractions of methane.

low pressure (below about 25 MPa) on the bubble curve lie nearly on the same line for different temperatures and diverge only at high pressure. Figure 4 shows that our data at 423 K are consistent with those reported by Sebastian et al. (1979).

Methane + 9,10-Dihydrophenanthrene Mixture. 9,-10-Dihydrophenanthrene (C_1) and methane (C_2) concentrations for this mixture at 423 and 463 K are reported in Table 2. Variations of 9,10-dihydrophenanthrene and methane concentrations with pressure are shown in Figures 5 and 6. Data for the gas phase at low pressures were not measurable for the same reason as above. The phase envelopes are shown in Figure 7. The agreement with the data of Sebastian et al. (1980) at 463 K in the liquid phase is good. As for the gas phase, it can be seen in Figure 8 that our data at high pressure are consistent with those

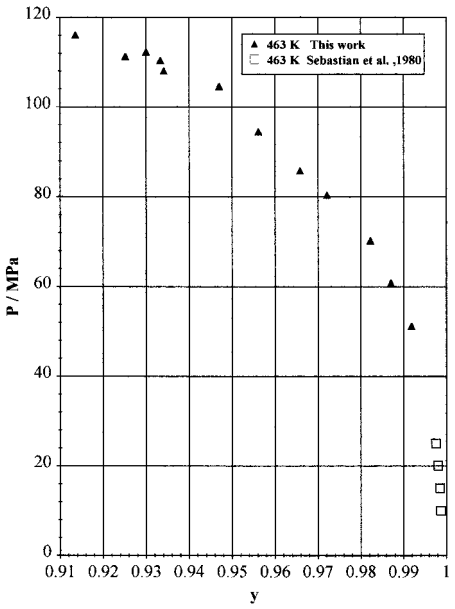

Figure 8. Comparison of gas-phase mole fractions of the mixture 9,10-dihydrophenanthrene + methane at 463 K (▲, this work; □, Sebastian et al. (1980)) on an appropriate scale. $y = C_2/(C_1 + C_2)$ = mole fraction of methane.

reported at lower pressures by Sebastian et al. (1980). Although it was possible to determine whole phase envelopes, the measurements near the critical points were more difficult. Again, the critical pressure decreases with increasing temperature though the temperature range is far from the 9,10-dihydrophenanthrene critical temperature (774 K). Both mixtures seem to have a similar behavior regarding this question and the same comment as above applies.

Conclusion

We have determined phase diagrams of the mixtures methane + tetralin and methane + 9,10 -dihydrophenanthrene at various temperatures. Other measurements on light + heavy hydrocarbon systems are in progress and will be published later.

List of Symbols

C_1 = concentration of the heavy component (tetralin or 9,10-dihydrophenanthrene)

C_2 = concentration of methane

P = pressure, MPa

T = temperature, K

x = mole fraction of methane in the liquid phase

y = mole fraction of methane in the gas phase

Literature Cited

Marteau, P.; Tobaly, P.; Ruffier-Meray, V.; Barreau, A. In Situ Determination of High Pressure Phase Diagrams of Methane-Heavy Hydrocarbon Mixtures Using an Infrared Absorption Method. *Fluid Phase Equilib.* **1996**, *119*, 213−230.

Marteau P.; Obriot, J.; Ruffier-Meray, V.; Behar, E. Experimental Determination of Phase Behavior of Binary Mixtures: Methane-Hexane and Methane-Benzene. *Fluid Phase Equilib.* **1997**, *129*, 285−305.

Marteau, P.; Tobaly, P.; Ruffier-Meray, V.; de Hemptinne, J. C. High Pressure Phase Diagrams of Methane + Squalane and Methane + Hexatriacontane Mixtures. *J. Chem. Eng. Data* **1998**, *43*, 362−366.

Sebastian, H. M.; Simnick, J. J.; Lin H.; Chao K. Gas−Liquid Equilibrium in Binary Mixtures of Methane with Tetralin, Diphenylmethane, and 1-Methylnaphthalene. *J. Chem. Eng. Data* **1979**, *24*, 149−152.

Sebastian, H. M.; Lin H.; Chao K. Gas−Liquid Equilibrium in Mixtures of Methane plus 9,10-Dihydrophenanthrene at Elevated Temperatures and Pressures. *J. Chem. Eng. Data* **1980**, *25*, 379−381.

Van Konynenburg, P. H.; Scott R. L. Critical Lines and Phase Equilibria in Binary van der Waals Mixtures *Philos. Trans. R. Soc. London* **1980**, *298*, 495−540.

Received for review February 9, 1999. Accepted July 8, 1999.

JE990045J